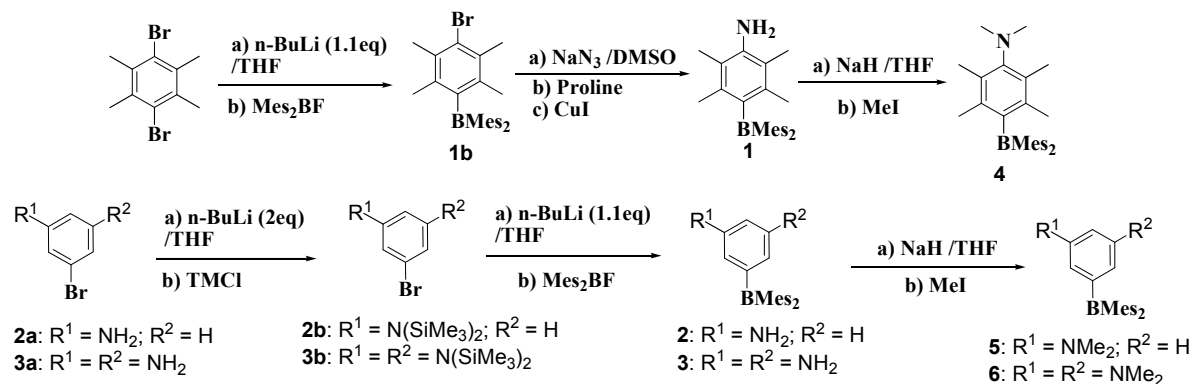


Supporting Information

**H-bond Assisted Mechanoluminescence of
Borylated Aryl Amines: Tunable Emission
and Polymorphism**

Pagidi Sudhakar, Kalluvettukuzhy K. Neena and Pakkirisamy Thilagar *

Synthesis



Scheme S1: Synthesis of compounds **1-6**

NMR Spectral Characterizations

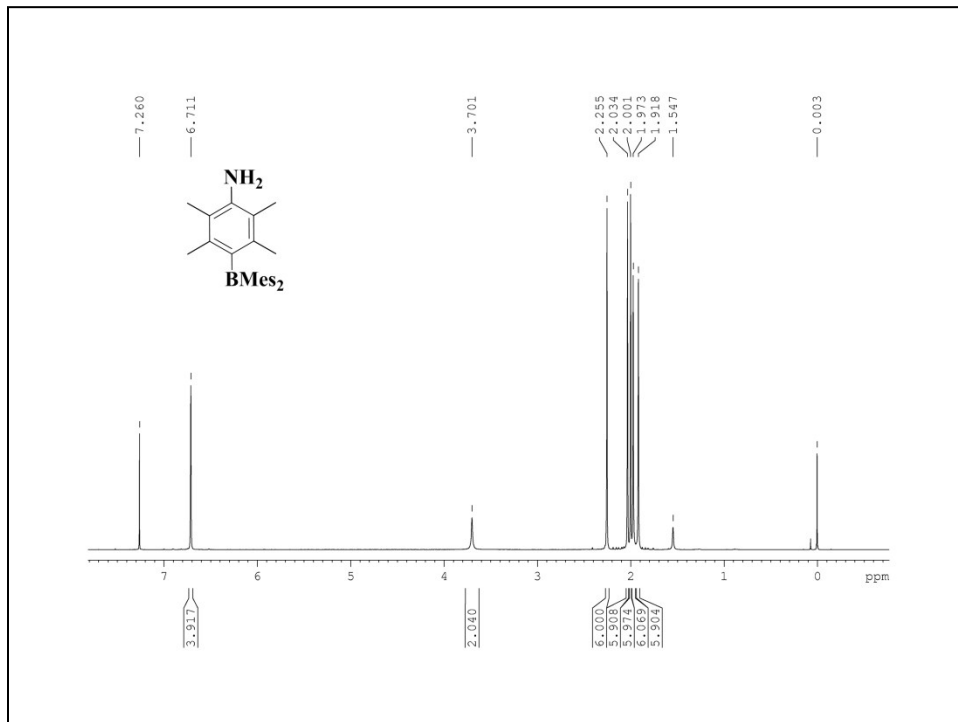


Figure S1: ¹H NMR spectrum of **1**

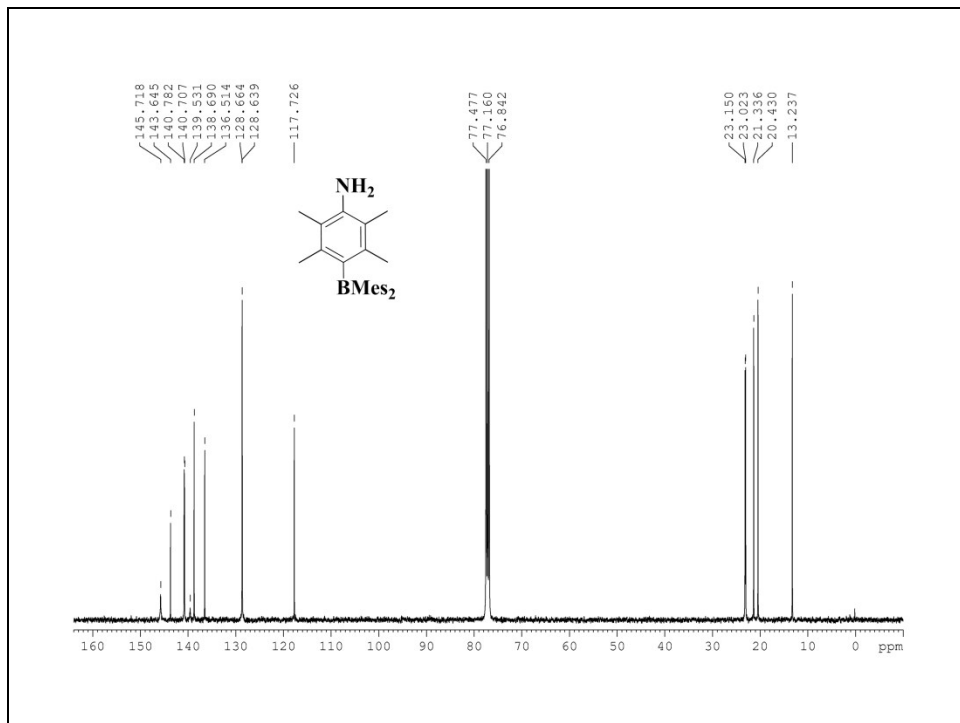


Figure S2: ^{13}C NMR spectrum of **1**

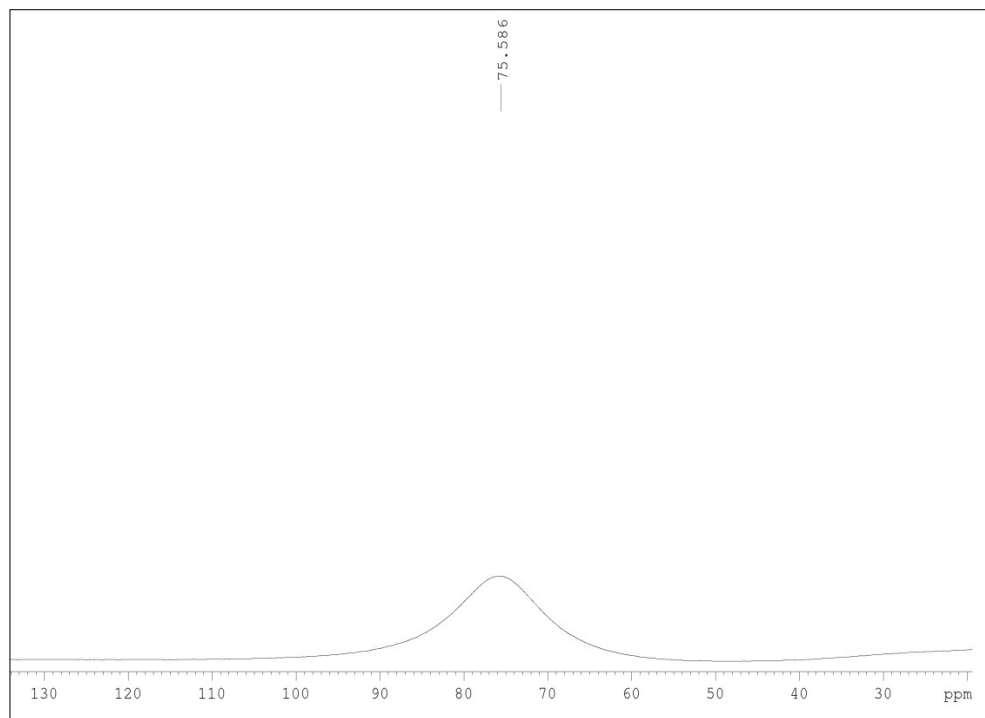


Figure S3: ^{11}B NMR spectrum of **1**

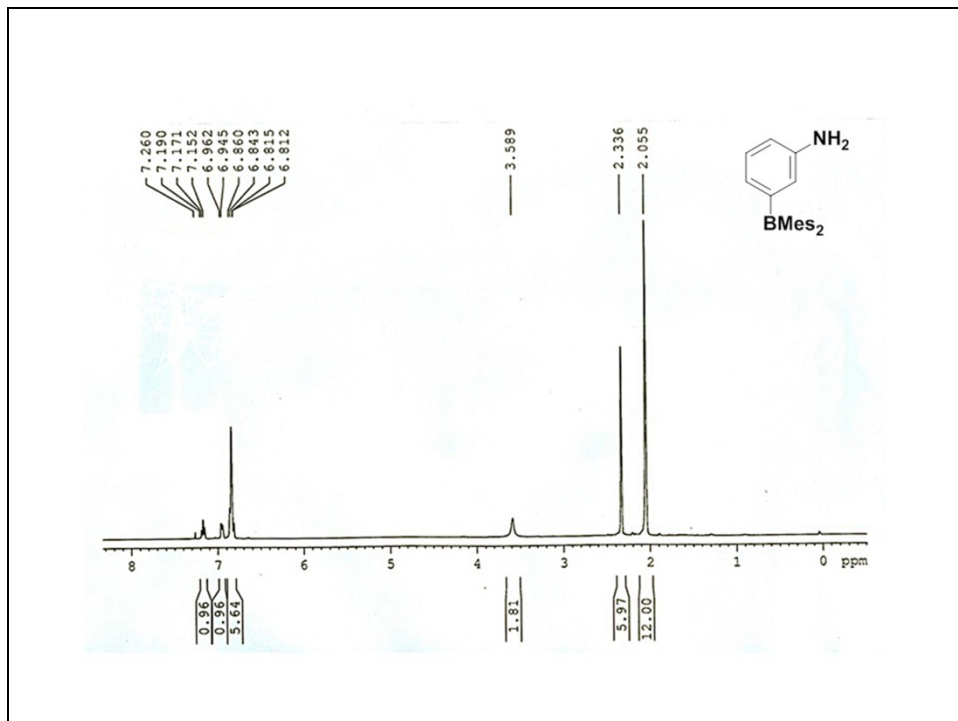


Figure S4: ¹H NMR spectrum of **2**

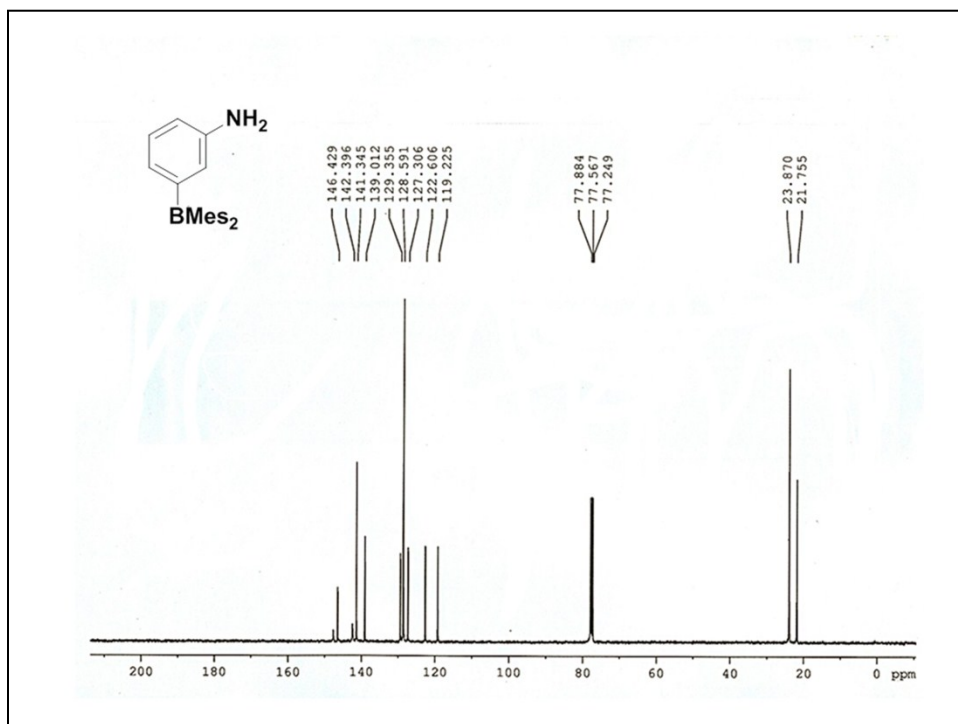


Figure S5: ¹³C NMR spectrum of **2**

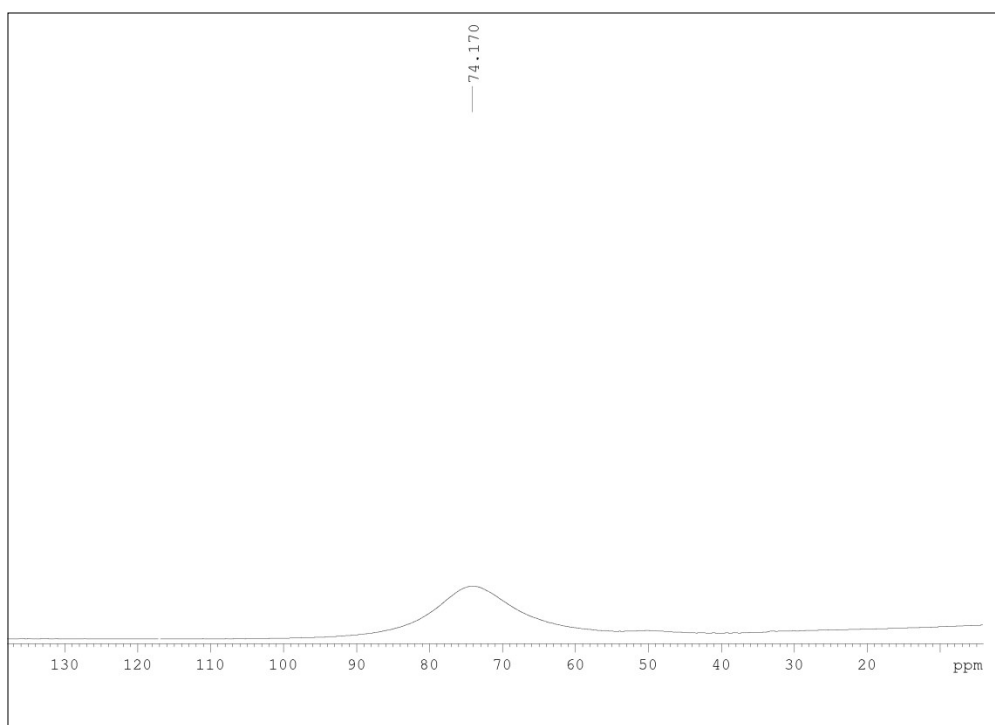


Figure S6: ^{11}B NMR spectrum of **2**

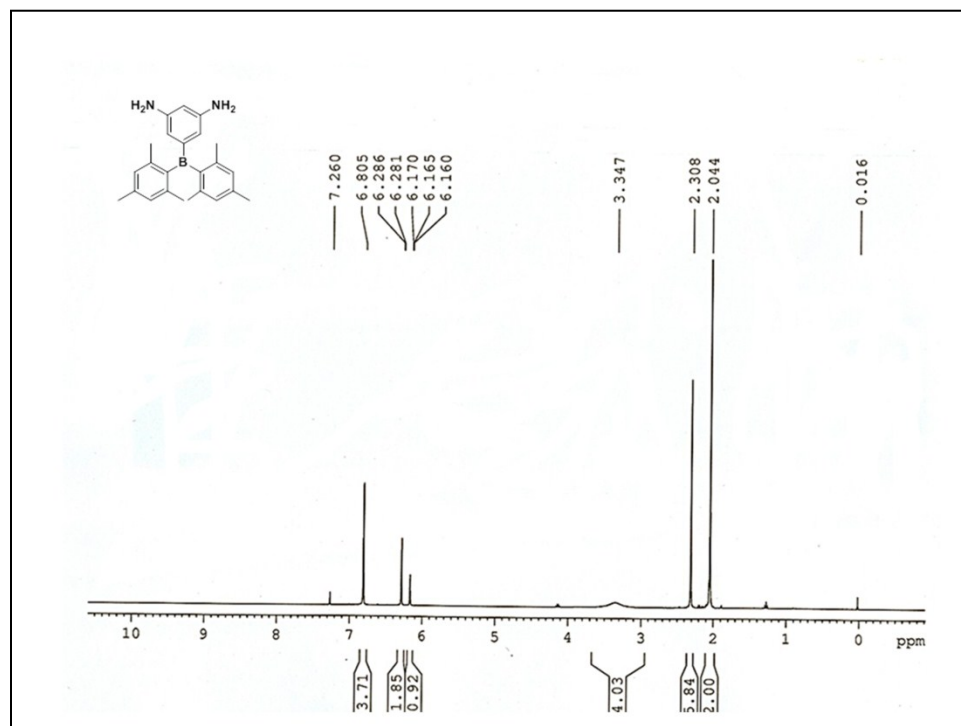


Figure S7: ^1H NMR spectrum of **3**

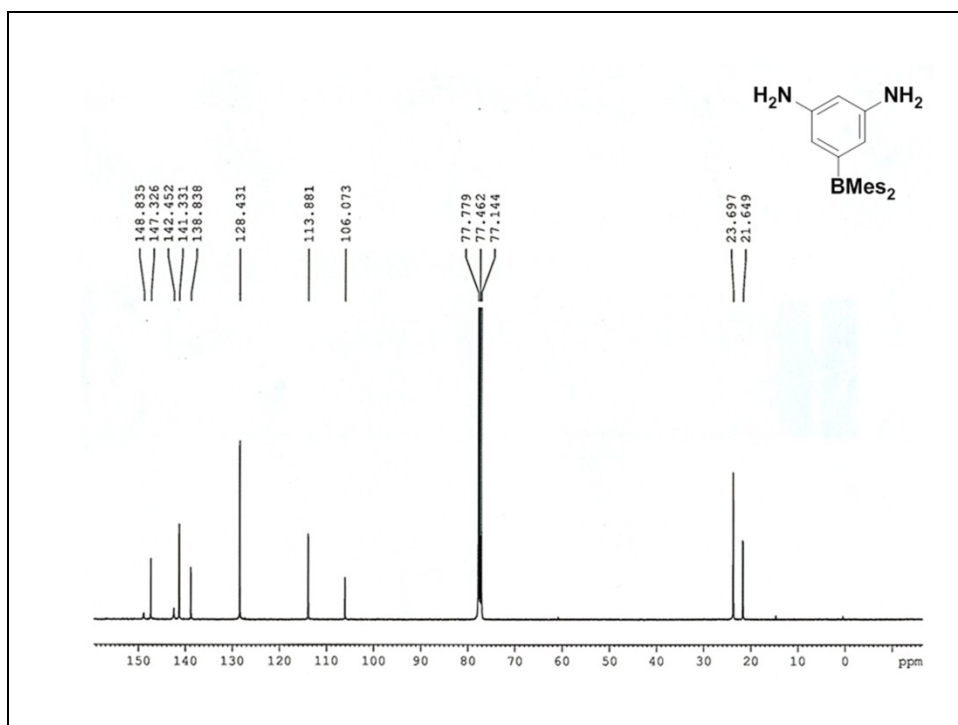


Figure S8: ^{13}C NMR spectrum of **3**

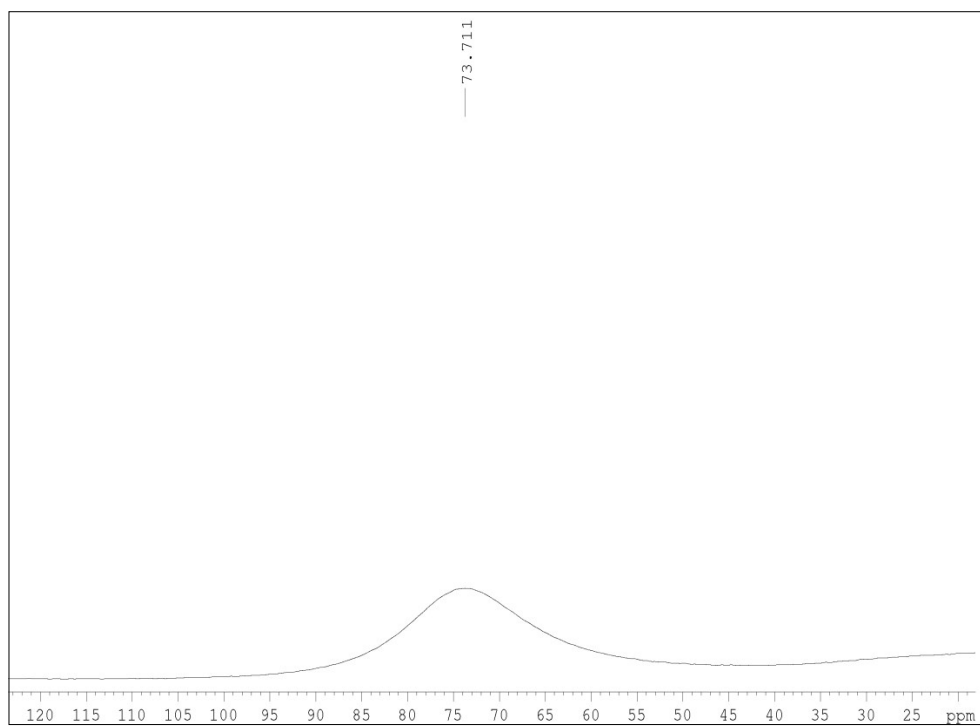


Figure S9: ^{11}B NMR spectrum of **3**

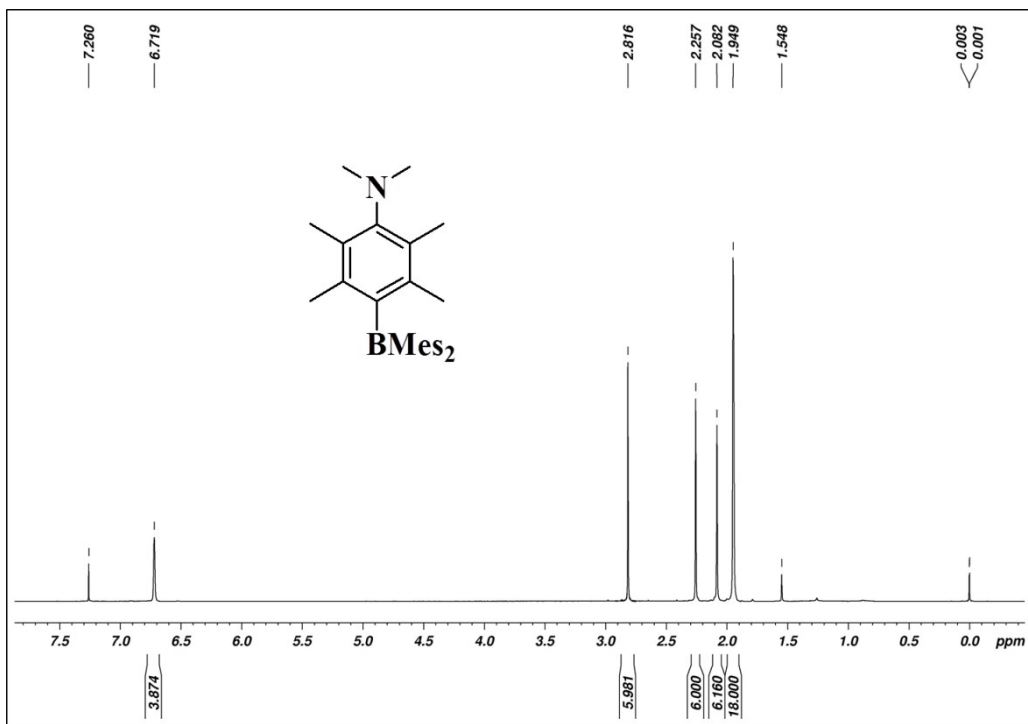


Figure S10: ¹H NMR spectrum of 4

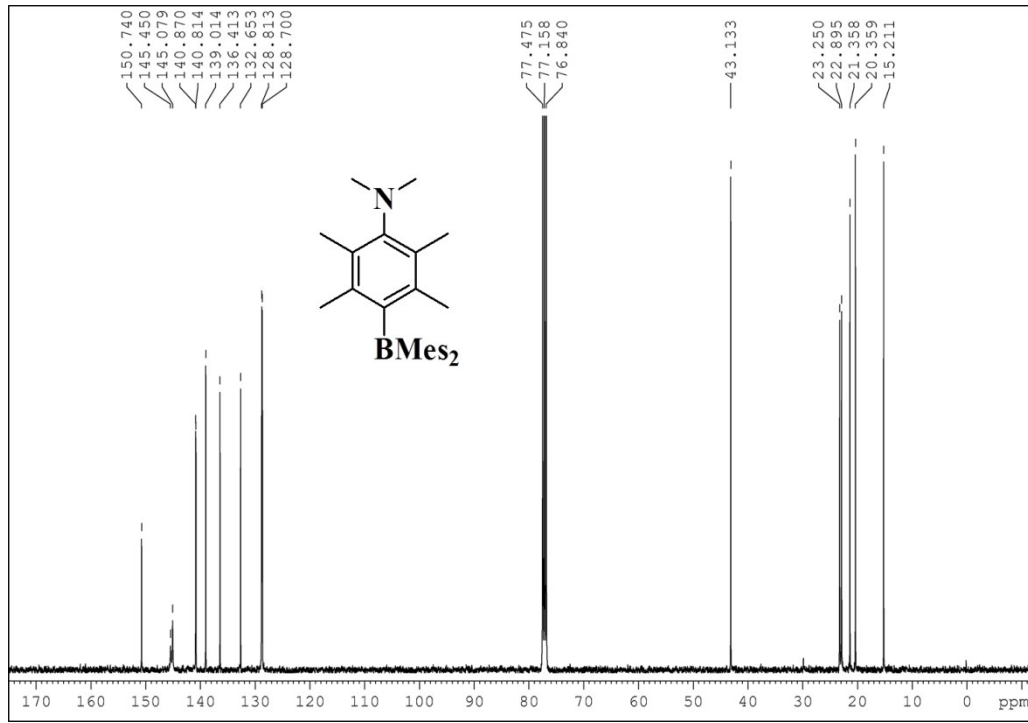


Figure S11: ¹³C NMR spectrum of 4

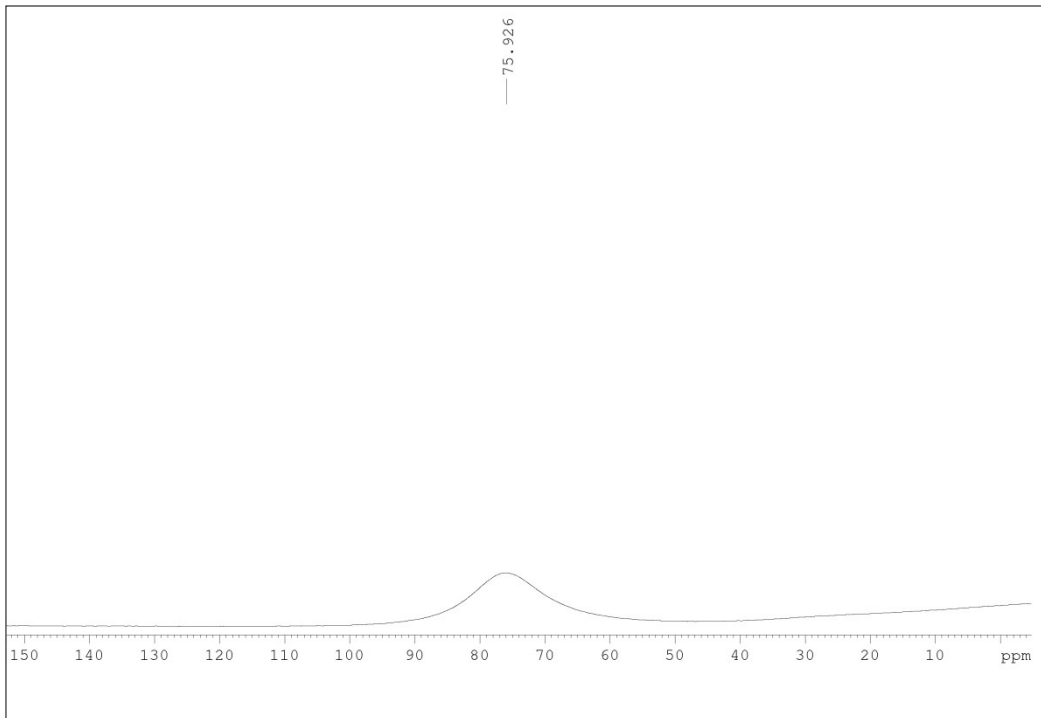


Figure S12: ^{11}B NMR spectrum of **4**

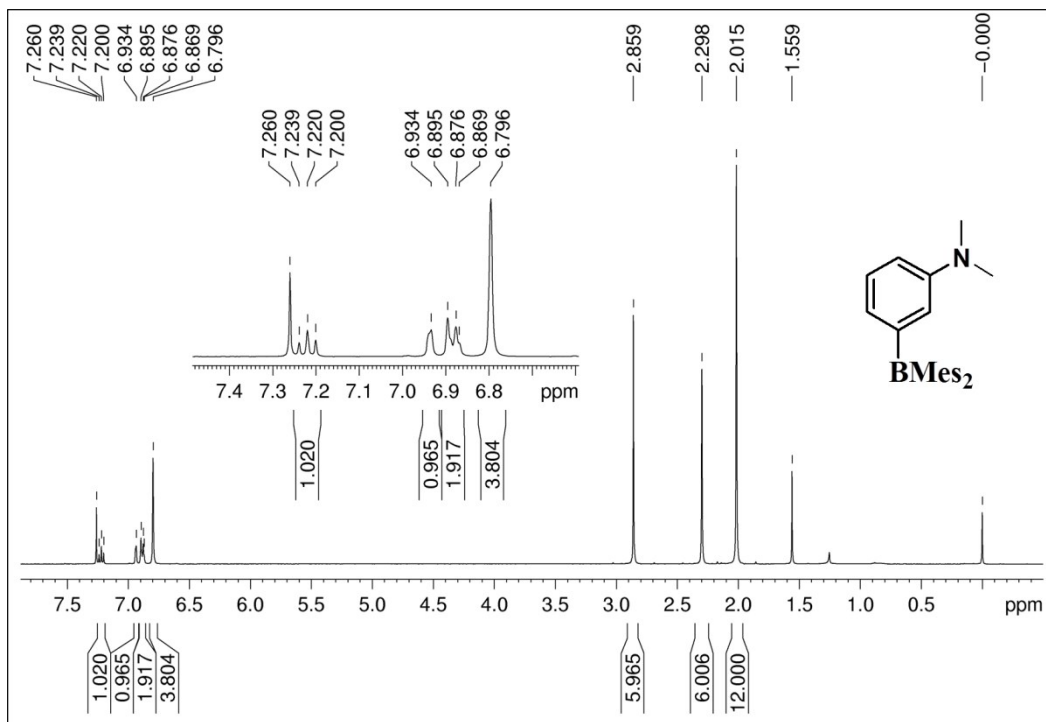


Figure S13: ^1H NMR spectrum of **5**

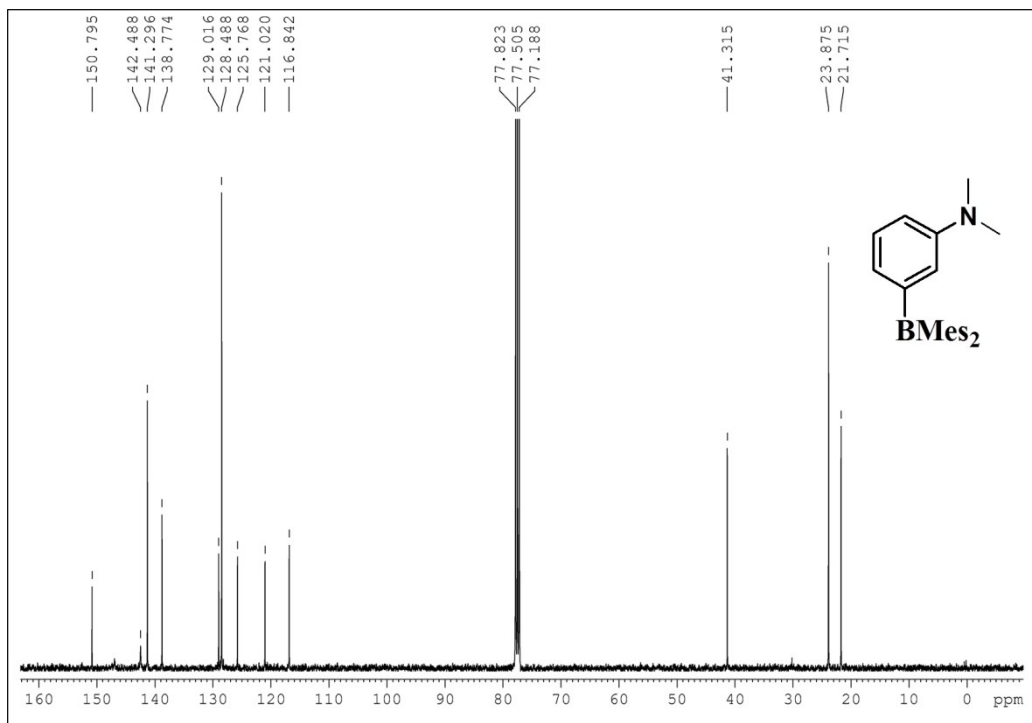


Figure S14: ^{13}C NMR spectrum of **5**

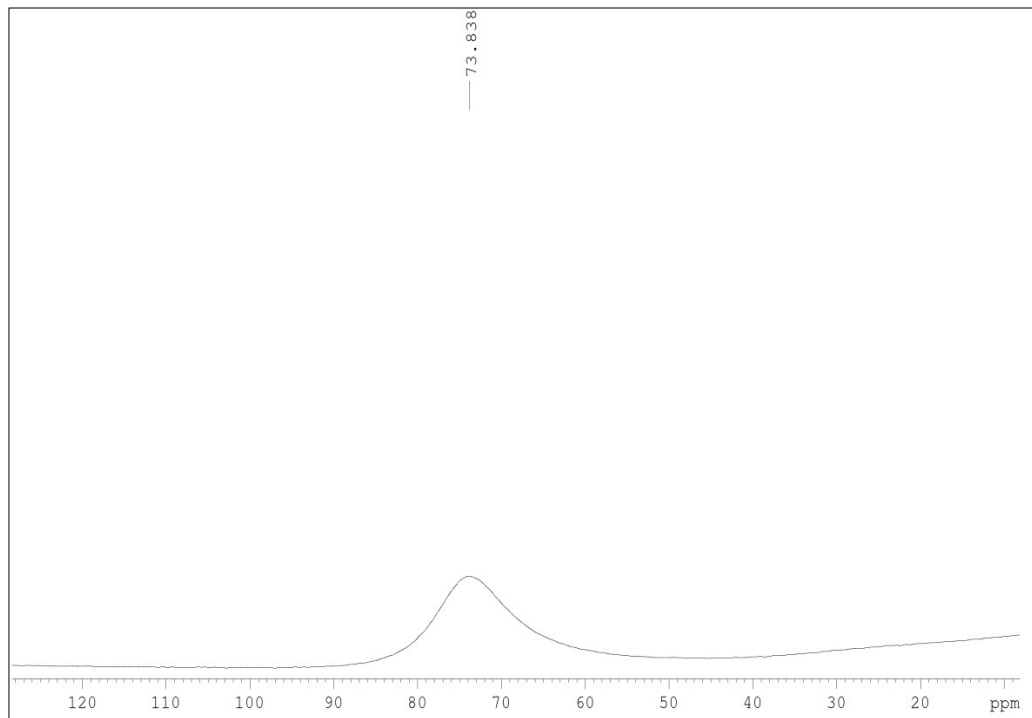


Figure S15: ^{11}B NMR spectrum of **5**

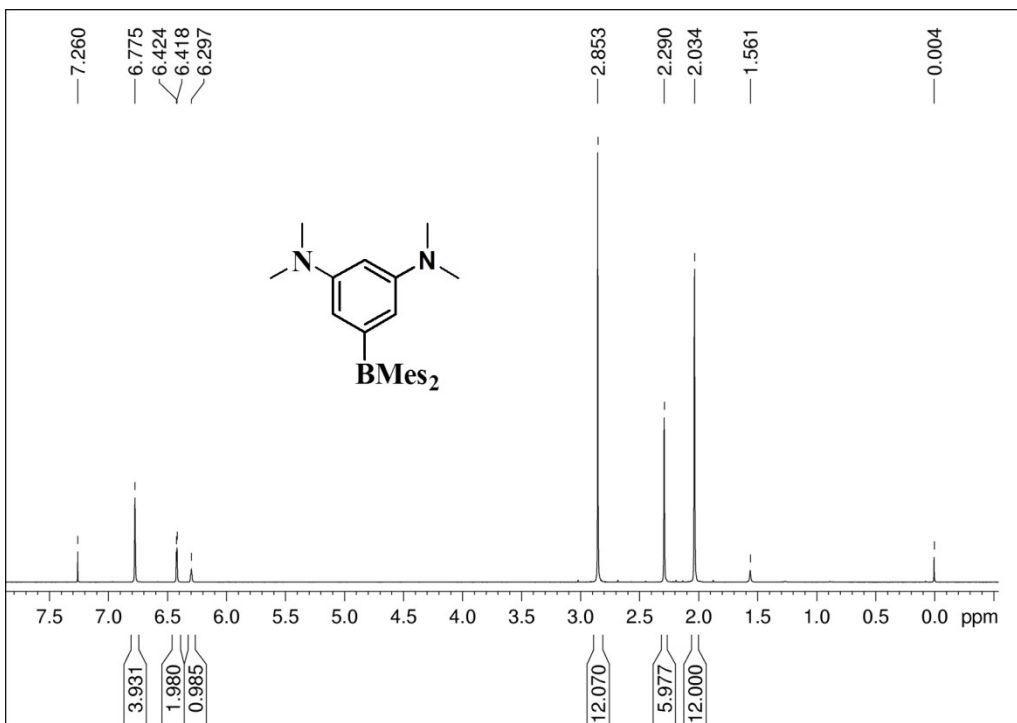


Figure S16: ^1H NMR spectrum of **6**

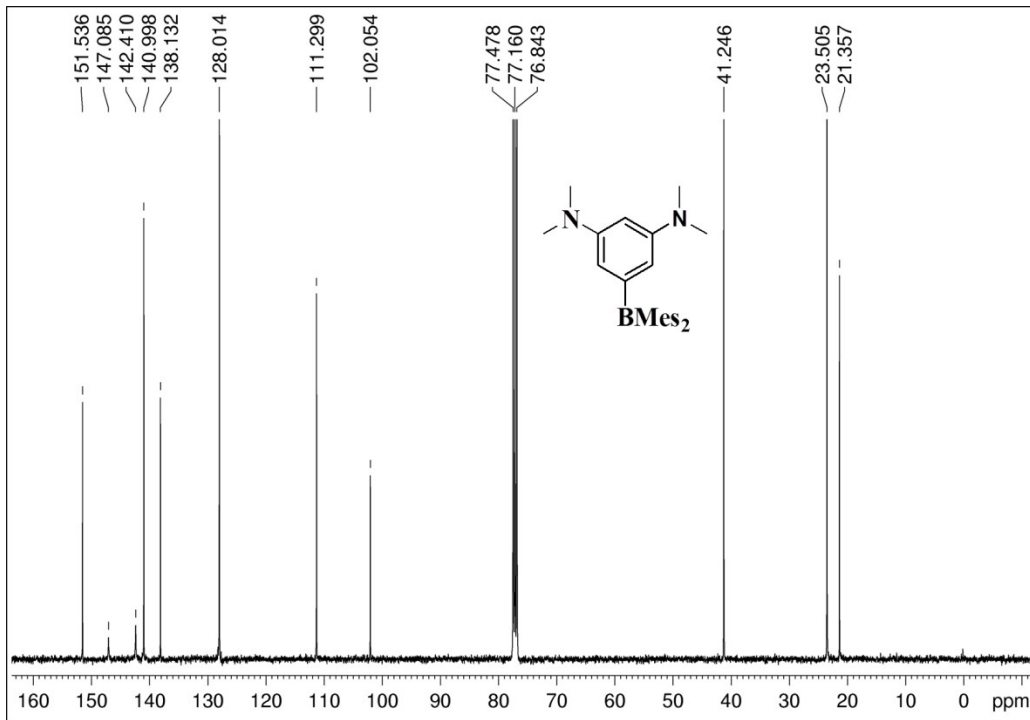


Figure S17: ^{13}C NMR spectrum of **6**

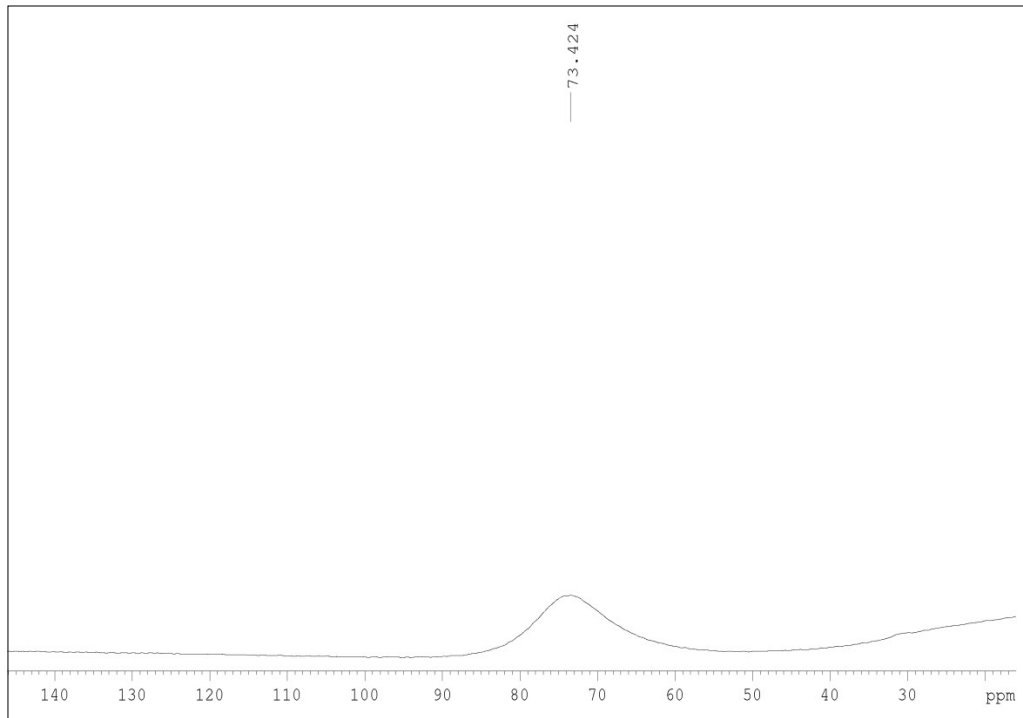


Figure S18: ¹¹B NMR spectrum of **6**

Mass Spectral Characterization

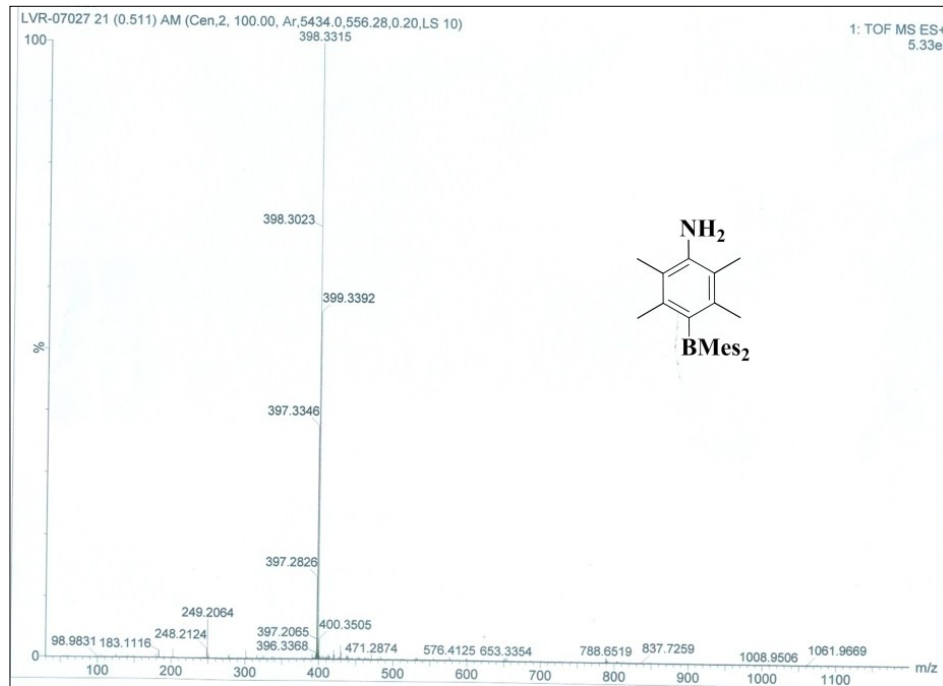


Figure S19: HRMS of **1**

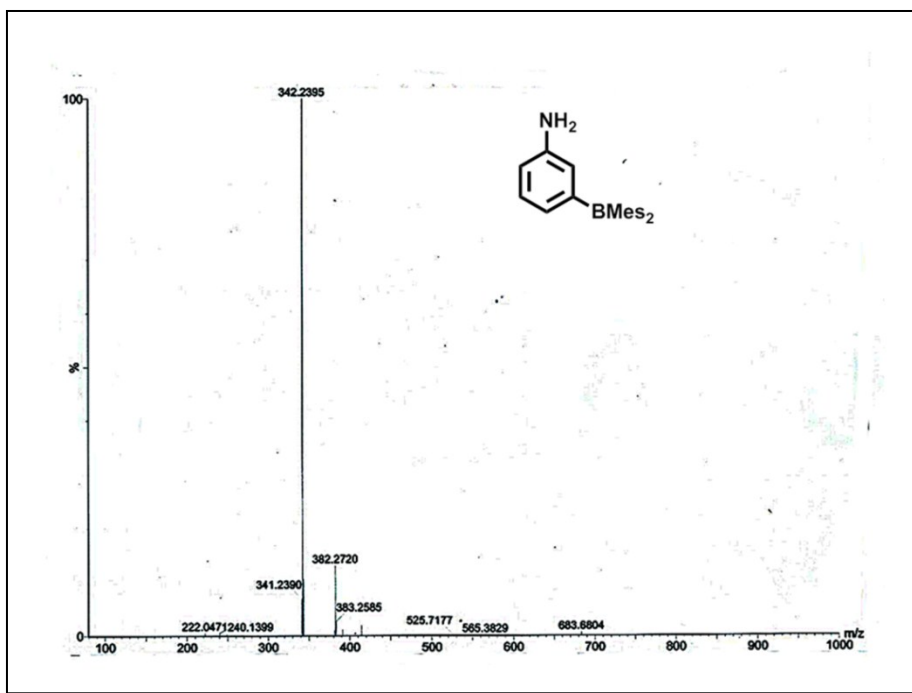


Figure S20: HRMS of 2

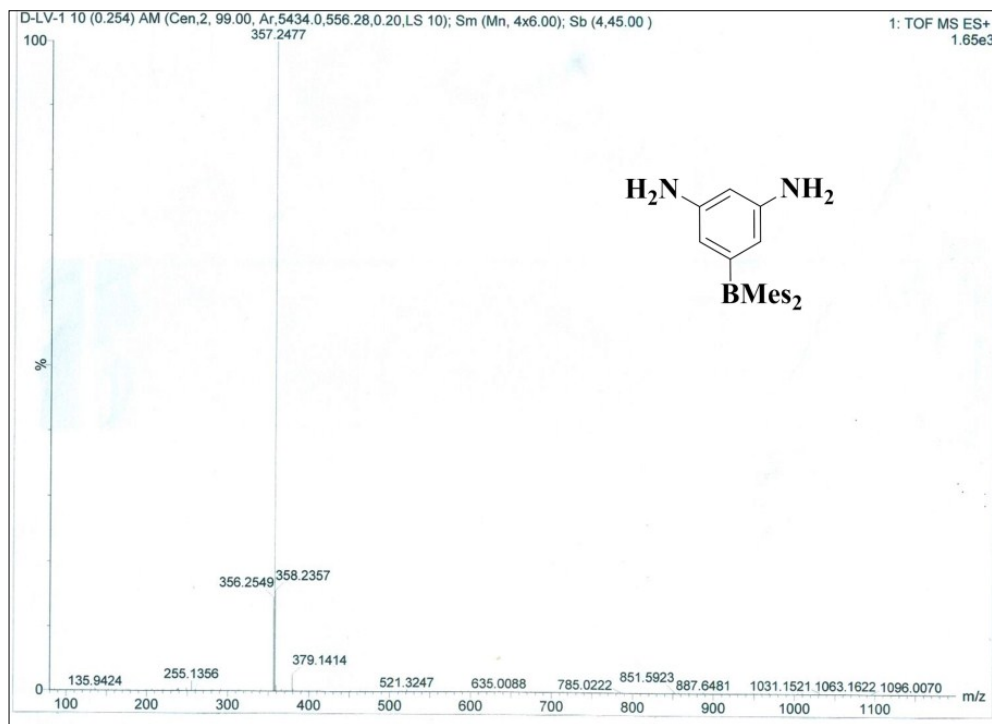


Figure S21: HRMS of 3

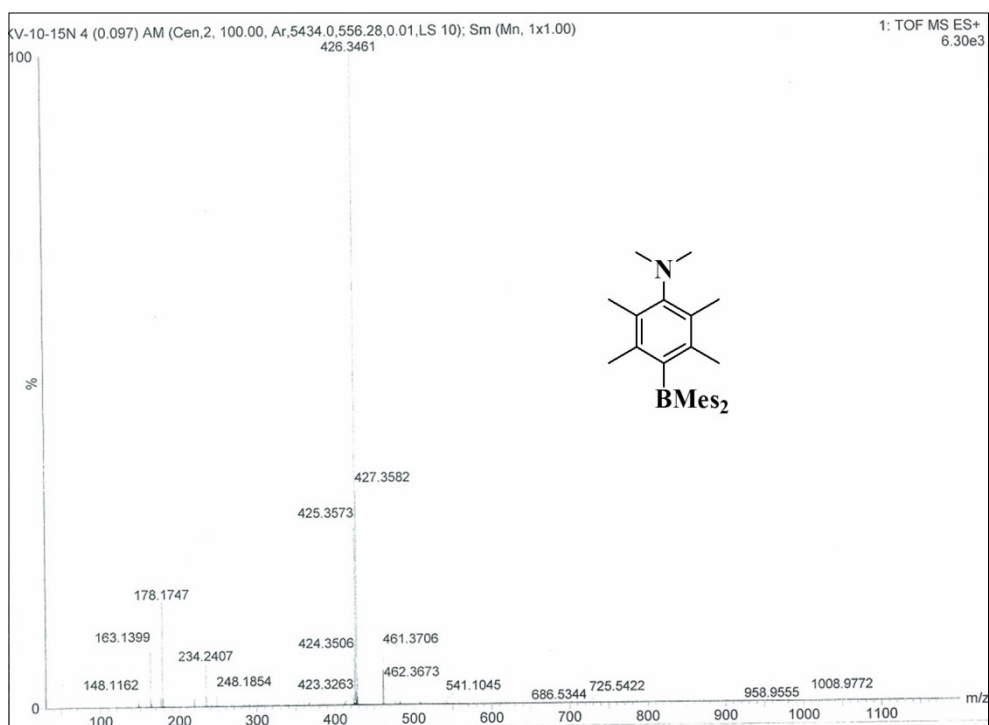


Figure S22: HRMS of 4

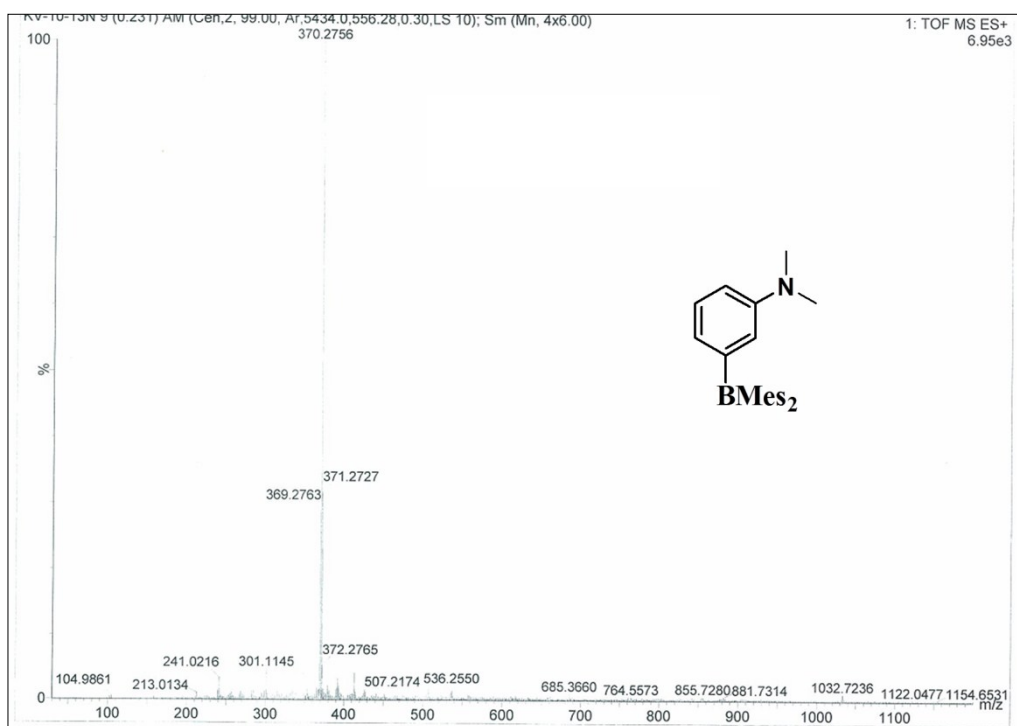


Figure S23: HRMS of 5

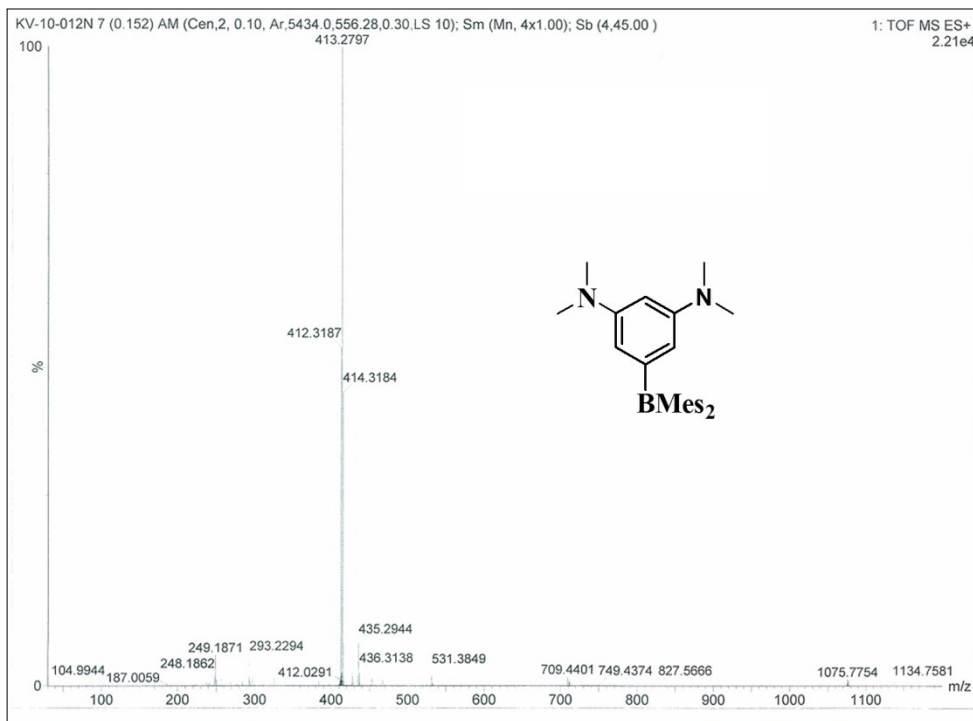


Figure S24: HRMS of **6**

Photophysical and Theoretical (DFT/TD-DFT) Studies

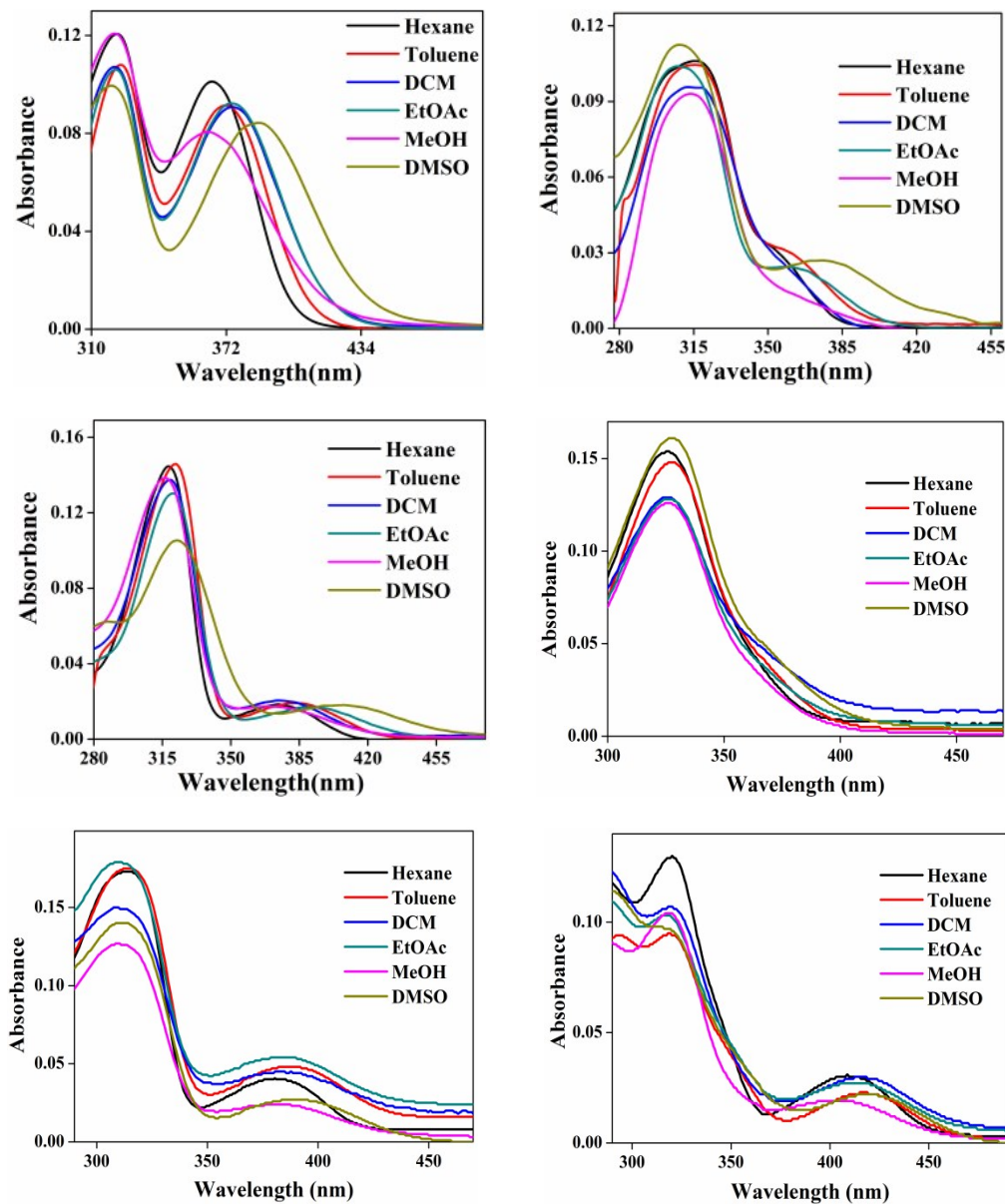


Figure S25: Absorption spectra of compounds **1** (top left), **2** (top right), **3** (middle left), **4** (middle right), **5** (bottom left) and **6** (bottom right) in solvents of different polarity (Conc. 10 μ M).

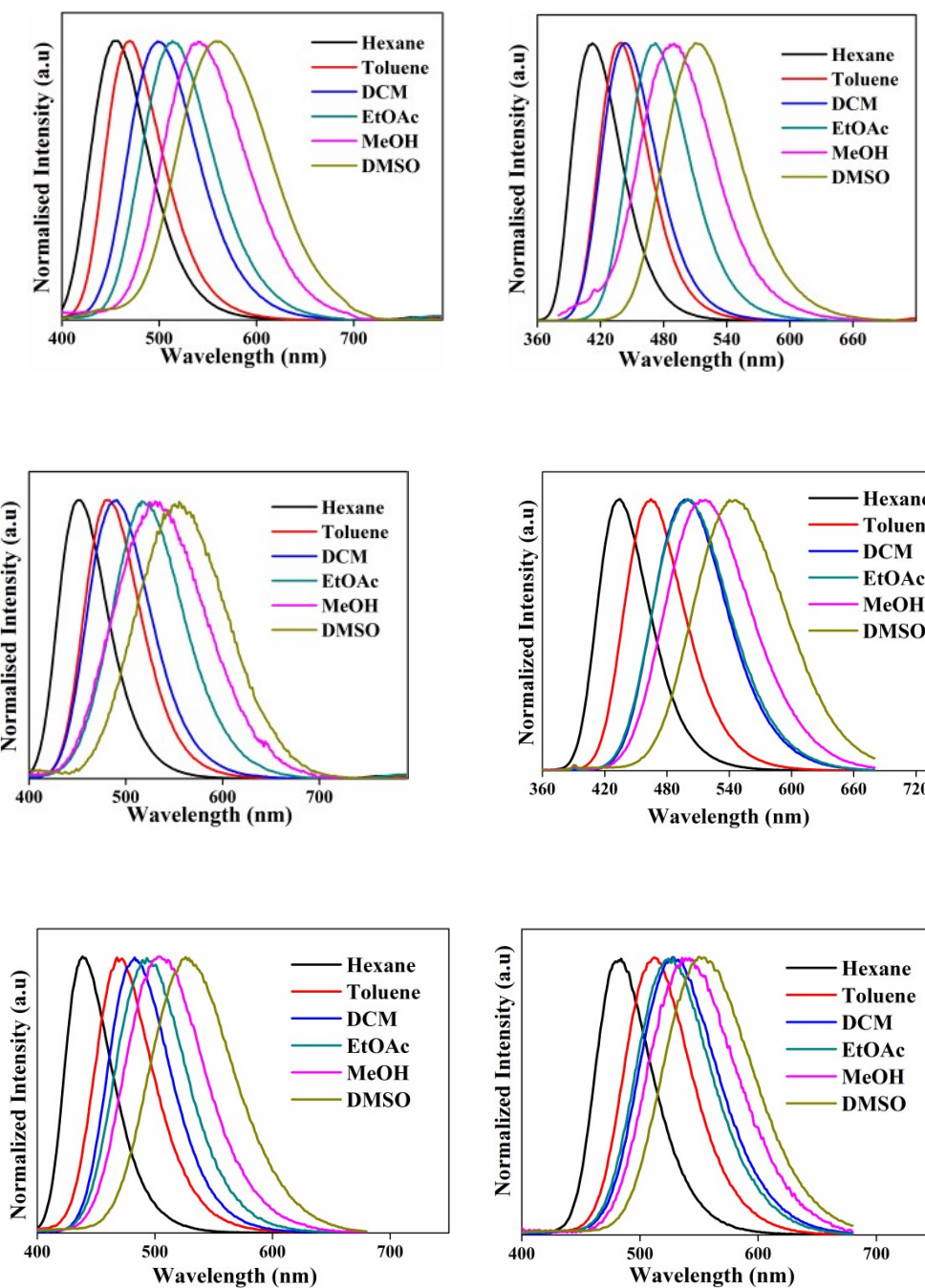


Figure S26: Emission spectra of compounds **1** (top left), **2** (top right), **3** (middle left), **4** (middle right), **5** (bottom left) and **6** (bottom right) in solvents of different polarity (Conc. 10 μ M, $\lambda_{\text{ex}} = 350$ nm).



Figure S27: Images of **1** (top left), **2** (top middle), **3** (top right), **4** (bottom left), **5** (bottom middle) and **6** (bottom right) in solvents of different polarity under UV light illumination ($\lambda_{\text{ex}} = 365 \text{ nm}$).

Table S1: UV-Vis absorption (λ_{abs}), fluorescence (λ_{em}), Stokes shifts and quantum yield (Φ_F) of borylamines **1**, **2**, **3**, **4**, **5** and **6** in solvents of different polarity (Conc. 10 μM , $\lambda_{\text{ex}} = 350 \text{ nm}$).

Compound No.	Solvent	λ_{abs} (nm); (ϵ , $\text{M}^{-1}\text{cm}^{-1}$)	λ_{em} (nm)	Stokes shift (cm^{-1})	Φ_F^{a}
1	Hexane	321(12101), 365 (10110)	455	5419	0.30
	Toluene	323(10830), 372(9180)	470	5605	0.50
	DCM	321(10685), 375(9063)	500	6667	0.55
	EtOAc	321(10685), 375(9247)	515	7249	0.28
	MeOH	321(12101), 364 (9080)	540	8954	0.08
	DMSO	319(9943), 386 (8402)	560	8050	0.03
2	Hexane	316(12014), 361(2673)	412	3429	0.20
	Toluene	355(3225), 315(11454)	439	5390	0.32
	DCM	315(10910)	443	9173	0.41
	EtOAc	360(2796), 310(11691)	472	6591	0.18
	MeOH	313 (9265)	490	11541	0.17
	DMSO	377(2495), 316(11006)	512	6993	0.23
	Hexane	374(1840), 318(14478)	451	4565	0.12

3	Toluene	383(1910), 321(14607)	481	5320	0.15
	DCM	375(2050), 319(13752)	489	6217	0.20
	EtOAc	392(1697), 320(13025)	517	6168	0.05
	MeOH	374 (1712), 317(13820)	531	7906	0.01
	DMSO	408(1805), 323(10509)	555	6492	0.02
4	Hexane	325 (15400)	435	7781	0.29
	Toluene	328 (14800)	464	8936	0.23
	DCM	327 (12900)	497	10460	0.29
	EtOAc	328 (12800)	500	10488	0.19
	MeOH	327 (12600)	512	11050	0.14
	DMSO	329 (16100)	540	11877	0.13
5	Hexane	316 (17300), 380 (4000)	438	3485	0.30
	Toluene	316 (17500), 392 (4800)	468	4143	0.18
	DCM	314 (14900), 392 (4400)	483	4806	0.21
	EtOAc	311 (17900), 390 (5400)	493	5357	0.10
	MeOH	310(12700), 387 (2400)	504	5999	0.22
	DMSO	314 (14000), 395 (2700)	529	6413	0.29
6	Hexane	320 (13000), 409 (3100)	484	3788	0.27
	Toluene	319 (9500), 419 (2300)	512	4335	0.45
	DCM	320 (10700), 418(3000)	528	4984	0.28
	EtOAc	319 (10300), 420 (2700)	528	4870	0.20
	MeOH	320 (10400), 422 (1600)	542	5246	0.15
	DMSO	315 (9800), 424 (2200)	551	5436	0.42

^a ($\Phi = \Phi_F \times (I/I_R) \times (A_R/A) \times (\eta^2/\eta_{R^2})$), where Φ = quantum yield, I = area under the curve of emission spectrum, A = absorbance, η = refractive index of solvent, quantum yield is calculated with reference to anthracene, $\Phi_F = 0.27$ in EtOH).

Table S2: Ground state and excited state dipole moment values of **1-6**

Compound No.	Dipole moment (Debye)		
	Ground state (μ_g) ^a	Excited state (μ_e)	$\Delta\mu = \mu_e - \mu_g$ ^b
1	1.87	13.34	11.47
2	1.91	16.83	14.92
3	1.88	11.96	10.08
4	0.35	14.39	14.04
5	2.22	13.02	10.80
6	2.54	11.20	8.66

a. obtained from DFT calculations; b. $\Delta\mu = (2\Delta\mu^2/hca_0^3)f(X) + A$, where $\Delta\mu$ is the electric dipole moment change upon electronic transition and h , c , a_0 , and A are the Planck's constant ($h = 6.626 \times 10^{-34} \text{ J s}$), speed of light ($c = 2.99 \times 10^8 \text{ m/s}$), Onsager radius of fluorophore and a constant.

Table S3: TRF data of Borylanilines **1, 2, 3, 4, 5** and **6** in different solvents (Conc. 10 μM , $\lambda_{\text{ex}} = 340$ nano-LED).

		Hexane	χ^2	DCM	χ^2	DMSO	χ^2
1	$\tau_1 (A_1, \%)$	4.22 (82)	1.0	13.45 (17)	1.1	6.77 (60)	1.0
	$\tau_2 (A_2, \%)$	6.00 (18)		20.61 (83)		8.55 (40)	
2	$\tau_1 (A_1, \%)$	3.72 (20)	1.1	3.62 (3)	1.2	2.97 (1)	1.1
	$\tau_2 (A_2, \%)$	8.80 (80)		23.81 (97)		35.63 (99)	
3	$\tau_1 (A_1, \%)$	4.51 (6)	1.1	2.20 (2)	1.1	2.60 (9)	1.1
	$\tau_2 (A_2, \%)$	10.76 (94)		32.45 (98)		14.13 (91)	
4	$\tau_1 (A_1, \%)$	1.72 (9)	1.0	1.91 (2)	1.1	7.27 (3)	1.1
	$\tau_2 (A_2, \%)$	3.34 (91)		17.31 (98)		21.42 (97)	
5	$\tau_1 (A_1, \%)$	6.76 (8)	1.0	2.00 (12)	1.1	11.30 (1)	1.1
	$\tau_2 (A_2, \%)$	12.00 (92)		36.23 (88)		50.17 (99)	
6	$\tau_1 (A_1, \%)$	7.60 (9)	1.0	11.84 (1)	1.2	6.78 (1)	1.1
	$\tau_2 (A_2, \%)$	12.42 (91)		35.80 (99)		50.13 (99)	

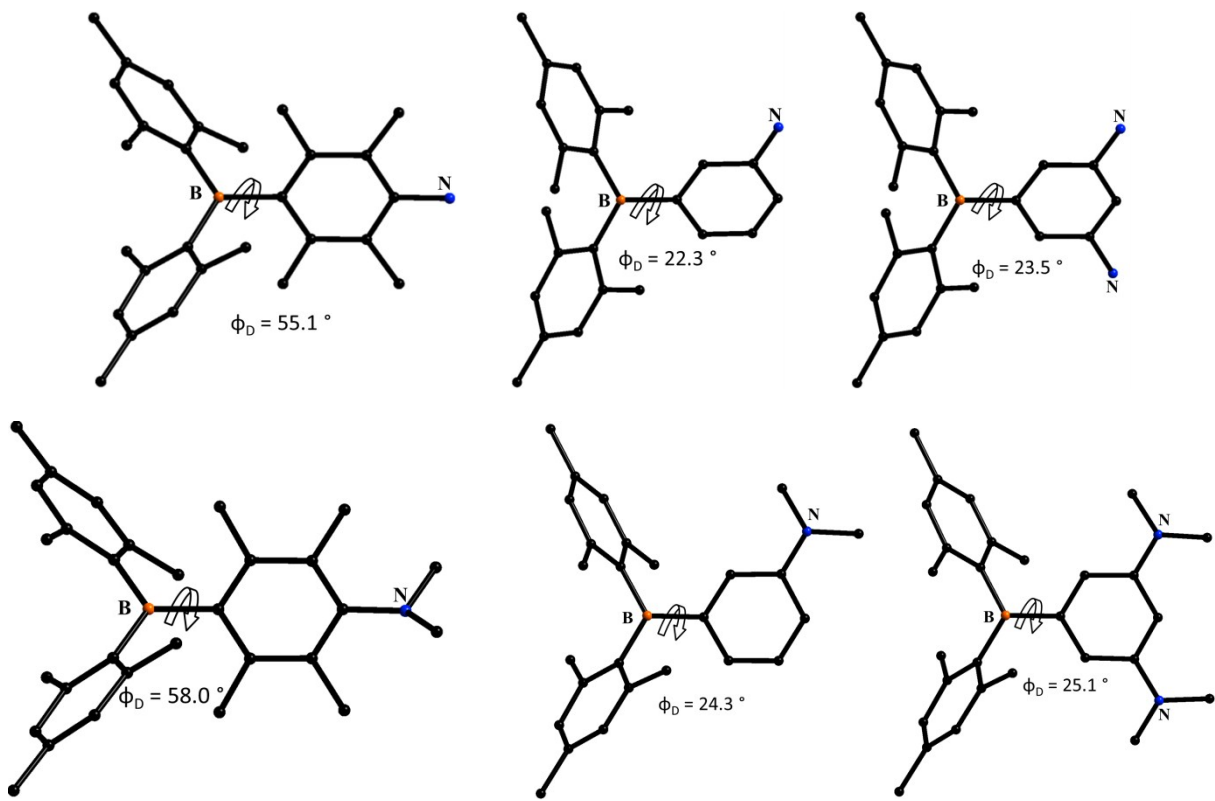


Figure S28: Ground state DFT optimized structures of **1**, **2**, **3**, **4**, **5** and **6** showing the dihedral angle between donor ($-\text{NH}_2$) and acceptor (TAB) plane (atom color codes: C-black, B-orange, N-blue, all the hydrogen atoms are removed for clarity).

Table S4: Selected bond Lengths (\AA) and torsion angles of **1**, **2**, **3**, **4**, **5** and **6** from the ground state DFT optimized structures.

Compound . No.	B-C(aryl)	B-C(Mes)	N-C(aryl) ^a	Torsion angle between BC2 plane and amine (°)
1	1.587	1.591	1.400	55.1
2	1.572	1.585	1.400	22.3
3	1.572	1.587	1.401	23.5
4	1.594	1.589	1.436	58.0
5	1.571	1.588	1.394	24.3
6	1.571	1.588	1.396	25.1

(aryl)^a = aniline/amine moiety

Table S5: Summary of dominant electronic transitions of compounds **1**, **2**, **3**, **4**, **5** and **6** obtained from TD-DFT calculations.

Compound	Excited State	E/eV	E/nm	f	Dominant transitions (percent contribution)
1	1	3.152	393.25	0.101	HOMO ->LUMO (98 %)
	2	3.715	333.66	0.128	HOMO-2 -> LUMO (89 %)
	3	3.750	330.63	0.004	HOMO-1 -> LUMO (89 %)
	4	3.997	310.14	0.029	HOMO-4 -> LUMO (87 %)
	5	4.035	307.27	0.002	HOMO-5 -> LUMO (46 %)
	6	4.104	302.04	0.050	HOMO-5 -> LUMO (50 %) HOMO-3 -> LUMO (42 %)
2	1	3.404	364.22	0.041	HOMO -> LUMO (98 %)
	2	3.648	339.86	0.091	HOMO-1 -> LUMO (97 %)
	3	3.811	325.26	0.025	HOMO-2 -> LUMO (97 %)
	4	3.871	320.24	0.050	HOMO-3 -> LUMO (98 %)
	5	3.945	314.26	0.013	HOMO-4 -> LUMO (98 %)
	6	4.621	268.28	0.085	HOMO-5 -> LUMO (86 %)
3	1	3.125	396.73	0.018	HOMO ->LUMO (99 %)
	2	3.692	335.78	0.091	HOMO-2 -> LUMO (98 %)
	3	3.769	328.90	0.132	HOMO-1 -> LUMO (72 %)
	4	3.890	318.65	0.023	HOMO-3 -> LUMO (75 %)
	5	3.979	311.54	0.013	HOMO-5 -> LUMO (88 %)
	6	4.036	307.17	0.002	HOMO-4 -> LUMO (63 %)
4	1	3.289	376.87	0.046	HOMO ->LUMO (96 %)
	2	3.613	343.14	0.008	HOMO-1 -> LUMO (98 %)
	3	3.669	337.85	0.125	HOMO-2 -> LUMO (97 %)
	4	3.753	330.36	0.0462	HOMO-3 -> LUMO (94 %)
	5	3.951	313.81	0.032	HOMO-4 -> LUMO (97 %)
	6	4.016	308.68	0.020	HOMO-5 -> LUMO (51 %)
5	1	3.110	398.61	0.025	HOMO -> LUMO (99 %)
	2	3.680	336.88	0.091	HOMO-1 -> LUMO (96 %)
	3	3.836	323.19	0.047	HOMO-2 -> LUMO (96 %)
	4	3.901	317.77	0.049	HOMO-3 -> LUMO (97 %)
	5	3.984	311.1	0.012	HOMO-4 -> LUMO (98 %)
	6	4.556	272.09	0.030	HOMO-4 -> LUMO (63 %)

6	1	2.849	435.06	0.021	HOMO -> LUMO (99 %)
	2	3.459	358.38	0.067	HOMO-1 -> LUMO (99 %)
	3	3.747	330.84	0.088	HOMO-2 -> LUMO (98 %)
	4	3.910	317.10	0.024	HOMO-3 -> LUMO (97 %)
	5	3.985	311.06	0.042	HOMO-4-> LUMO (97 %)
	6	4.053	305.91	0.013	HOMO-4-> LUMO (98 %)

Table S6: Solid state luminescence properties of compounds **1**, **2**, **3**, **4**, **5** and **6** ($\lambda_{\text{ex}} = 350$ nm for emission spectral measurements and 340 nano-LED for TRF measurements).

	λ_{em} (nm)	Φ_F (%)	Life time, τ (ns)				$K_r \times 10^6$ (S ⁻¹) ^b	$K_{nr} \times 10^6$ (S ⁻¹) ^b
			τ_1 (A1, %)	τ_2 (A2, %)	τ^a	χ^2		
1	446	10.7	5.30 (68)	11.42 (32)	7.26	1.11	14.74	123.00
2	443	22.2	7.23 (13)	19.11 (87)	17.57	1.09	12.64	44.28
3	469	40.3	3.46 (6)	23.75 (94)	22.53	1.16	17.88	26.50
4	437	29.9	4.97 (49)	9.00 (51)	7.03	1.13	42.53	99.72
5	452	31.0	3.95 (5)	25.62 (95)	24.54	1.42	12.63	28.12
6	504	38.6	7.02 (11)	24.61 (89)	22.68	1.11	17.02	22.07

^aaverage life time, $\tau = \{ (A1\tau_1 + A2\tau_2)/100 \}$; ^b following equations have been used for the calculation of K_r and K_{nr} ; $\{ \phi_F = k_r/(k_r+k_{nr}) \}$ and $\{ \tau = 1/(k_r+k_{nr}) \}$, where ϕ_F is the absolute fluorescence quantum yield at solid state measured using a calibrated integrating sphere setup, τ is the average life time and k_r and k_{nr} are the radiative non-radiative (k_{nr}) decay rate constants, respectievly.⁴

Molecular Structure

Table S7: Selected crystallographic data and for structures **3BP** and **3GP**

	3BP	3GP
Empirical formula	C ₂₄ H ₂₉ B ₁ N ₂	C ₂₄ H ₂₉ B ₁ N ₂
Formula weight	356.30	356.30
Temperature(K)	100(2)	100(2)
Wavelength/ Å	0.71073	0.71073
Crystal System	Monoclinic	Triclinic
Space group	P21/c	P-1
a/ Å	8.654(1)	8.423(3)
b/ Å	12.191 (1)	15.808(6)
c/ Å	39.327(1)	16.730(6)
α [°]	90	99.825(2)
β [°]	98.715(1)	101.361(2)
γ [°]	90	100.190(2)
V/Å ³	4149.40(9)	2100.50(1)
Crystal size (mm)	0.07 x 0.08 x 0.10	0.05 x 0.09 x 0.14
Z	4	4
Crystal density, g cm ⁻³	1.13	1.13
[a]R _{all} , R _{obs}	0.081, 0.056	0.052, 0.044
[b]wR _{2_all} , wR _{2_obs}	0.148, 0.136	0.125, 0.120
Collected reflns	58331	33986
Unique reflns	8126	8257
Theta range for data collection	1.8 to 26.0°	1.6 to 25.0°
Absorption coefficient	0.065 mm ⁻¹	0.065 mm ⁻¹
Goodness-of-fit on F ²	1.076	1.064
CCDC number	1407288	947986

$$^{[a]}R_1 = \sum \left| |F_o| - |F_c| \right| / \sum |F_o| . ^{[b]}wR_2 = [\sum \{w(F_o^2 - F_c^2)^2\} / \sum \{w(F_o^2)^2\}]$$

Table S8: Selected bond lengths [\AA] and angles [°] for conformers (**3BP-A** and **3BP-B**) and for conformers (**3GP-A** and **3GP-B**)

Compound No.	Important bond lengths[\AA]			Important bond angles(°)	Important torsion angles(°)
	B-C(aryl) ^a	B-C(Mes)	N-C(aryl) ^a		
3BP-A	1.564	B1-C7=1.585 B1-C16=1.578	N1-C3=1.390 N2-C5=1.401	C7-B1-C16=124.87 C16-B1-C1=119.55 C1-B1-C7=115.58	C16-B1-C1-C6=33.92 C7-B1-C1-C2=31.56
3BP-B	1.567	B2-C31=1.578 B2-C40=1.585	N3-C27=1.405 N4-C29=1.390	C31-B2-C40=121.37 C40-B2-C25=117.60 C31-B2-C25=120.83	C40-B2-C25-C30=36.25 C31-B2-C25-C26=38.69
3GP-A	1.570	B1-C7=1.578 B1-C16=1.584	N1-C5=1.398 C3-N2=1.400	C7-B1-C16=125.08 C16-B1-C1=115.59 C1-B1-C7=119.31	C16-B1-C1-C6=21.66 C7-B1-C1-C2=21.77
3GP-B	1.567	B2-C40=1.581 B2-C31=1.578	N3-C27=1.410 N4-C29=1.406	C40-B2-C31=123.61 C31-B2-C25=118.86 C25-B2-C40=117.50	C40-B2-C25-C30=21.29 C31-B2-C25-C26=22.77

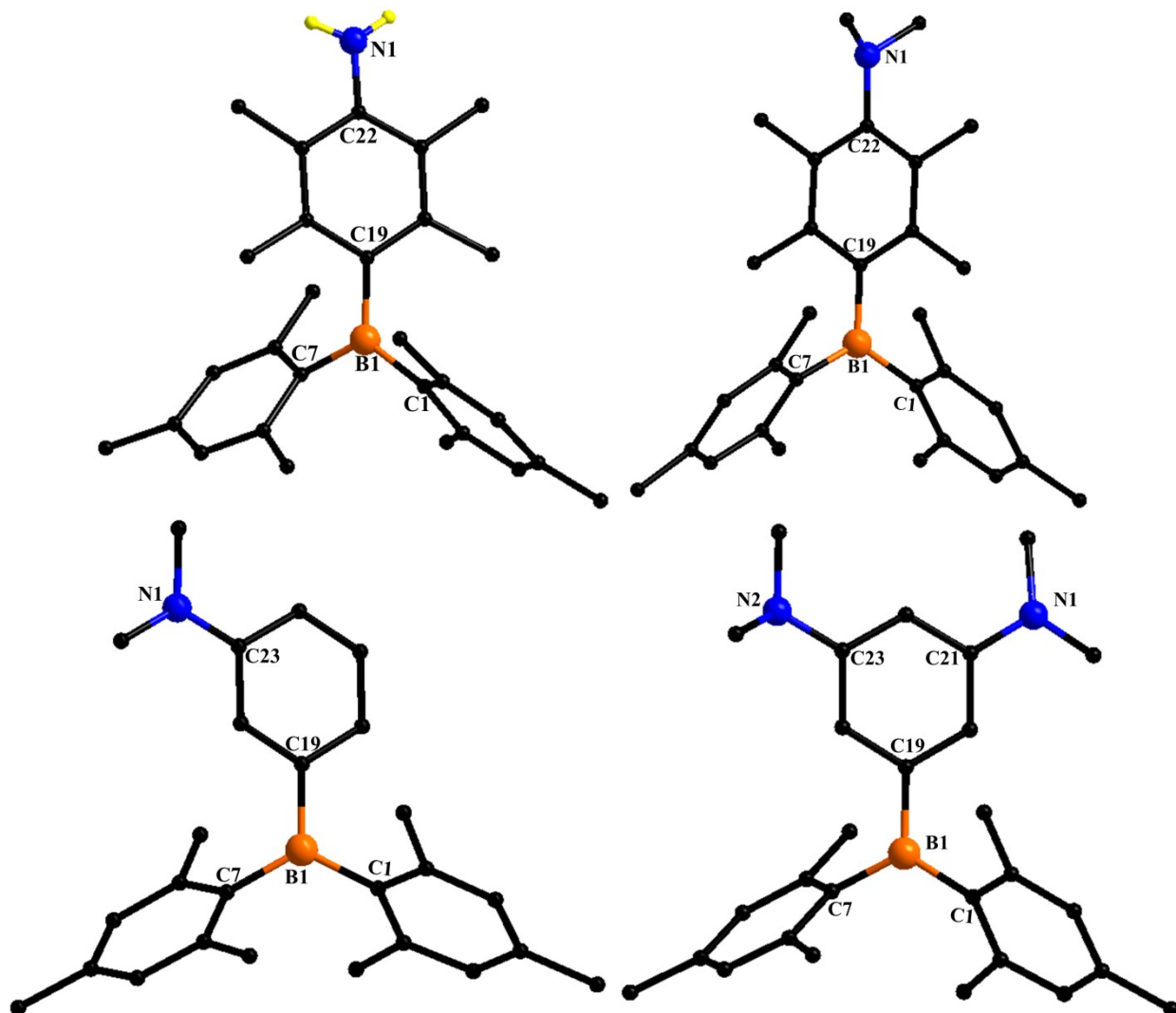
(aryl)^a = aniline moiety

Table S9: Selected crystallographic data and for structures **1**, **4**, **5** and **6**

	1	4	5	6
Empirical formula	C ₂₈ H ₃₆ B ₁ N ₁	C ₃₀ H ₄₀ B ₁ N ₁	C ₂₆ H ₃₂ B ₁ N ₁	C ₂₈ H ₃₇ B ₁ N ₂
Formula weight	397.39	425.44	369.34	412.41
Temperature(K)	373 K	298 K	298 K	298 K
Wavelength/ Å	0.71073 Å	0.71073	0.71073	0.71073
Crystal System	Orthorhombic	Triclinic	Triclinic	Triclinic
Space group	<i>Pbca</i>	<i>P-1</i>	<i>P-1</i>	<i>P-1</i>
a/ Å	8.488(4)	7.881(4)	8.490(2)	8.843(2)
b/ Å	16.546(7)	11.540(7)	11.754(3)	12.238(3)
c/ Å	32.812(1)	15.256(8)	12.334(3)	12.790(3)
α [°]	90.00	75.470(18)	106.332(13)	73.939(8)
β [°]	90.00	87.554(18)	96.924(13)	71.148(8)
γ [°]	90.00	78.835(18)	102.979(12)	75.050(8)
V/Å ³	4608.7(4)	1317.6(1)	1128.6(5)	1237.0(6)
Crystal size (mm)	0.20*0.17*0.10	0.15* 0.10* 0.08	0.20* 0.15* 0.10	0.15* 0.10* 0.07
Z	8	2	2	2
Crystal density, g cm ⁻³	1.15	1.072	1.087	1.107
[a]R _{all} , R _{obs}	0.073, 0.047	0.141, 0.085	0.083, 0.065	0.078, 0.065
[b]wR _{2_all} , wR _{2_obs}	0.111, 0.103	0.238, 0.224	0.204, 0.192	0.219, 0.208
Collected reflns	137931	40525	17830	45261
Unique reflns	4037	4640	3973	4362
Theta range for data collection	2.97 to 25.00°	3.0 to 25.0°	1.8 to 25.0°	3.3 to 25.0°
Absorption coefficient	0.064 mm ⁻¹	0.060 mm ⁻¹	0.061 mm ⁻¹	0.063 mm ⁻¹
Goodness-of-fit on F ²	1.019	1.181	1.269	1.084
CCDC number	1530085	1530086	1530087	1530088

$$[a]R_1 = \sum \left| |F_o| - |F_c| \right| / \sum |F_o| . [b]wR_2 = [\sum \{w(F_o^2 - F_c^2)^2\} / \sum \{w(F_o^2)^2\}]$$

Table S10: Selected bond lengths [\AA] and angles [$^\circ$] for **1**, **4**, **5** and **6** from the crystal structures

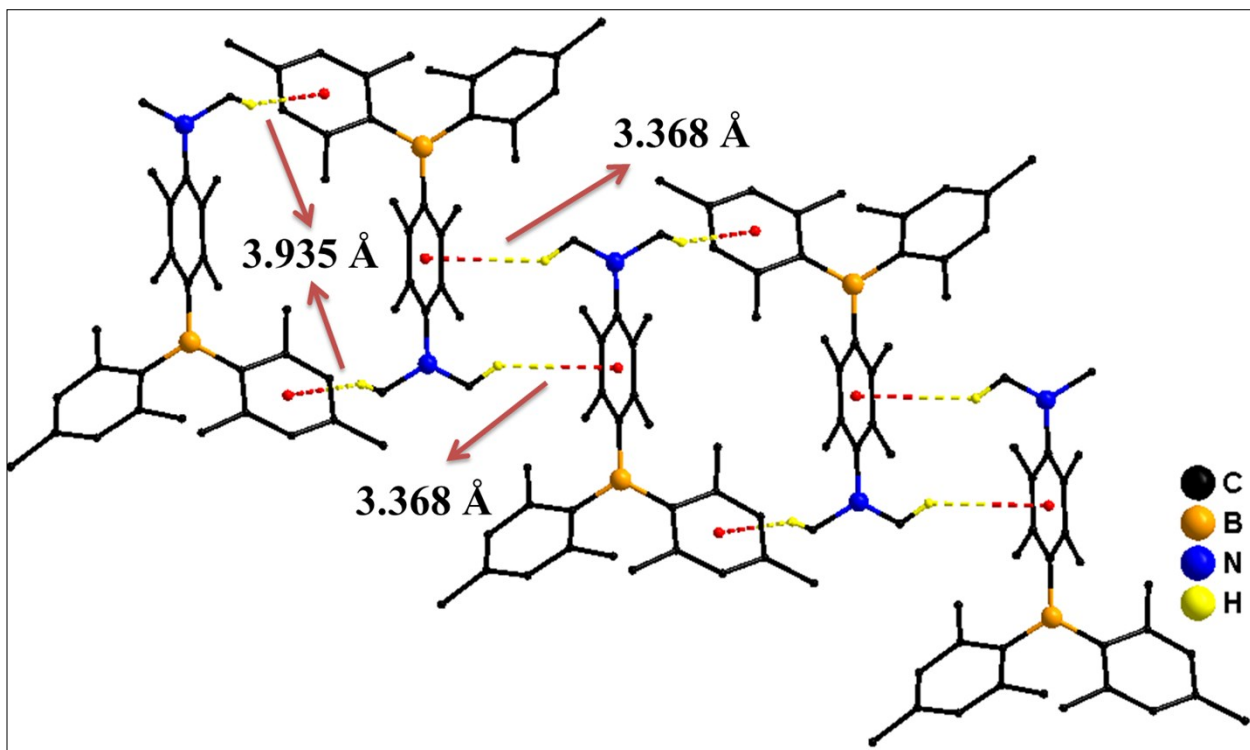


Molecular structures of **1** (top left), **4** (top right), **5** (bottom left) and **6** (bottom right) showing the atom numbering schemes.

Compound No.	Important bond lengths [\AA]			Important bond angles ($^\circ$)	Torsion angle between BC2 plane and amine ($^\circ$)
	B-C(aryl) ^a	B-C(Mes)	N-C(aryl) ^a		
1	B1-C19= 1.581(3)	B1-C1= 1.585(3)	N1-C22= 1.389 (2)	C7-B1-C1=120.6 (1) C19-B1-C1= 117.0(1) C19-B1-C7= 122.4(1)	53.7(2)

5	B1-C19= 1.586(5)	B1-C1= 1.599(6)	N1-C22= 1.438 (4)	C7-B1-C1= 119.8 (3) C19-B1-C1= 119.7(3) C19-B1-C7= 120.5(3)	59.2(5)
5	B1-C19= 1.566(3)	B1-C1= 1.567 (3)	N1-C23= 1.390(3)	C7-B1-C1= 124.0 (2) C19-B1-C1= 118.9 (2) C19-B1-C7= 117.1(2)	29.9(3)
6	B1-C19= 1.570(3)	B1-C1= 1.581(3)	N1-C21= 1.413(4)	C7-B1-C1= 123.9(2)	38.8 (3)
	B1-C7= 1.570(4)		N2-C23= 1.390(2)	C19-B1-C1= 116.2(2) C19-B1-C7= 119.9 (2)	

(aryl)^a = aniline/amine moiety



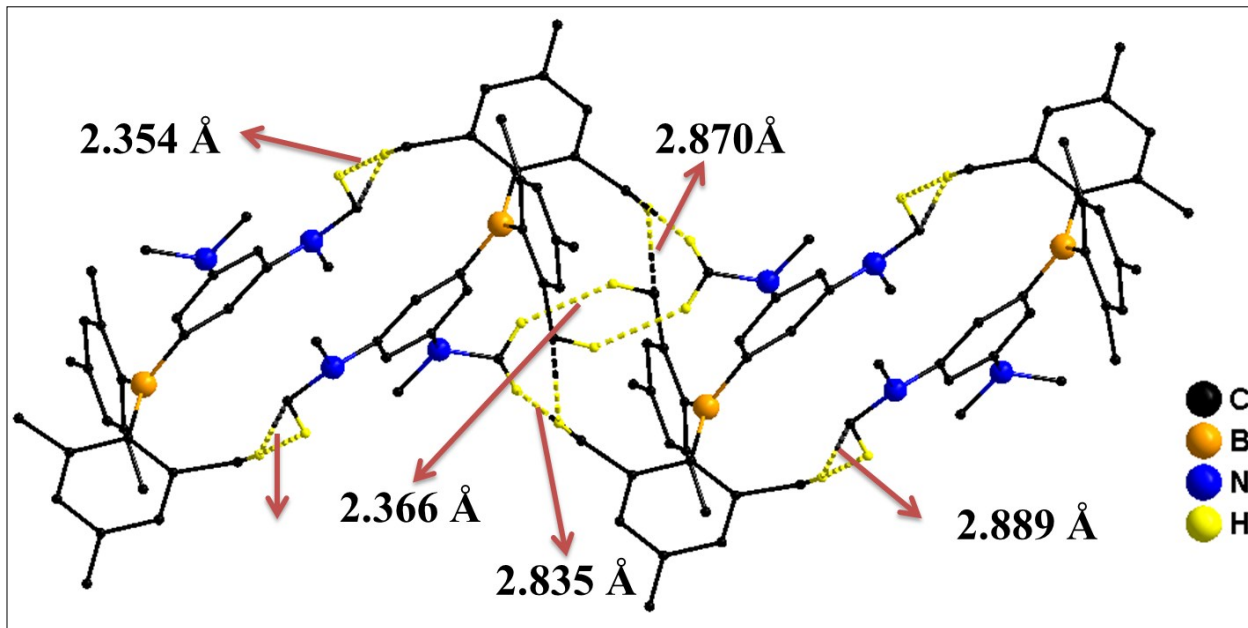
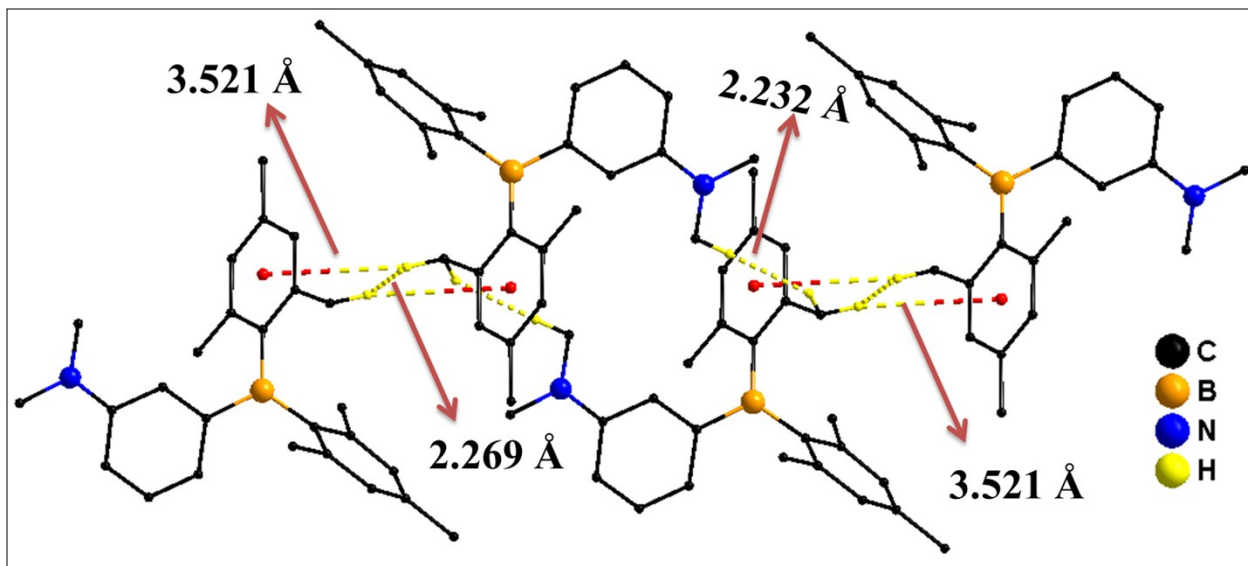


Figure S29: Intermolecular interaction diagram of **4** (top), **5** (middle) and **6** (bottom).

Mechanochromic Characteristics

Table S11: Mechanochromic luminescence properties of compound **1** and **3** ($\lambda_{\text{ex}} = 350$ nm for emission spectral measurements and 340 nano-LED for TRF measurements).

	λ_{em} (nm)	Φ_F (%)	Life time, τ (ns)				$K_r \times 10^6$ (S ⁻¹) ^b	$K_{nr} \times 10^6$ (S ⁻¹) ^b
			τ_1 (A1, %)	τ_2 (A2, %)	τ^a	χ^2		
1	446	10.7	5.30 (68)	11.42 (32)	7.26	1.11	14.74	123.00
1G	465	12.2	4.30 (27)	12.97 (73)	10.63	1.14	11.48	82.60
3	469	40.3	3.46 (6)	23.75 (94)	22.53	1.16	17.88	26.50
3G	493	36.5	4.76 (9)	27.08 (91)	25.07	1.33	14.55	25.33

^a average life time, $\tau = \{ (\text{A1}\tau_1 + \text{A2}\tau_2)/100 \}$; ^b following equations have been used for the calculation of K_r and K_{nr} ; $\{ \phi_F = k_r/(k_r+k_{nr}) \}$ and $\{ \tau = 1/(k_r+k_{nr}) \}$, where ϕ_F is the absolute fluorescence quantum yield at solid state measured using a calibrated integrating sphere setup, τ is the average life time and k_r and k_{nr} are the radiative non-radiative (k_{nr}) decay rate constants, respectievly.⁴

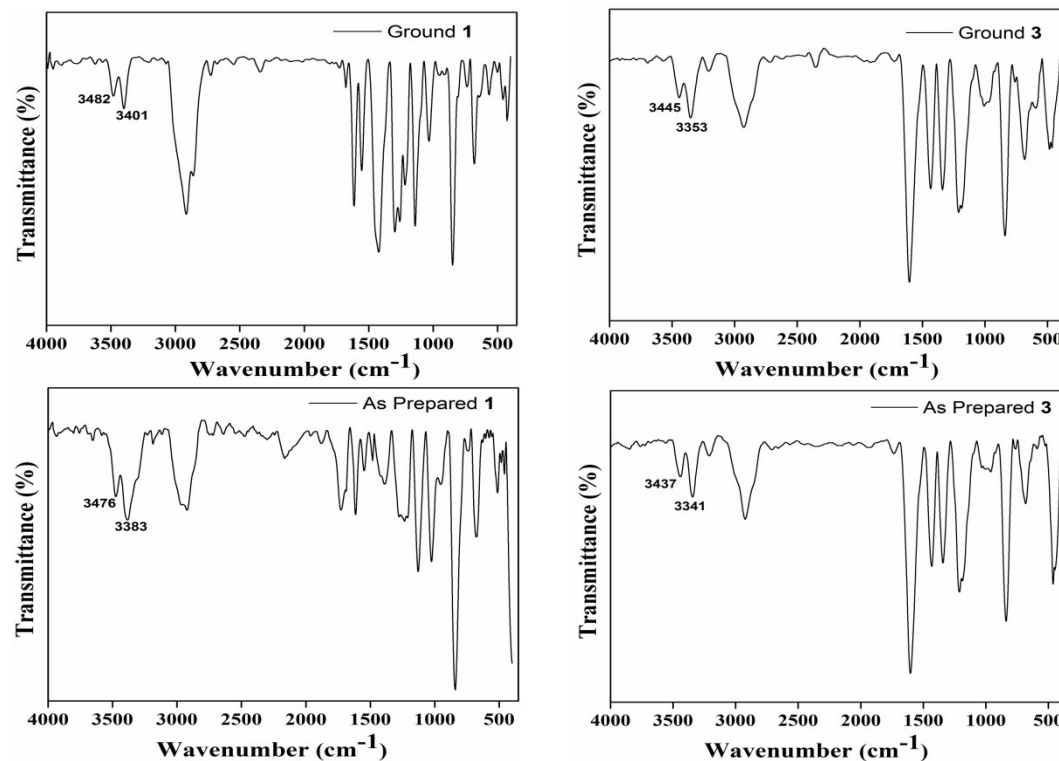


Figure S30: IR spectra of different samples of **1** (left) and **3** (right) obtained after mechanical grinding (Pristine sample (bottom) and Ground samples (bottom)).